

Towards Autonomous and Safe Last-mile Deliveries with AI-augmented Self-driving Delivery Robots

Eyad Shaklab*, Areg Karapetyan*, Arjun Sharma, Murad Mebrahtu, Mustofa Basri, Mohamed Nagy, Majid Khonji, and Jorge Dias

Abstract—In addition to its crucial impact on customer satisfaction, last-mile delivery (LMD) is notorious for being the most time-consuming and costly stage of the shipping process. Pressing environmental concerns combined with the recent surge of e-commerce sales have sparked renewed interest in automation and electrification of last-mile logistics. To address the hurdles faced by existing robotic couriers, this paper introduces a customer-centric and safety-conscious LMD system for small urban communities based on AI-assisted autonomous delivery robots. The presented framework enables end-to-end automation and optimization of the logistic process while catering for real-world imposed operational uncertainties, clients' preferred time schedules, and safety of pedestrians. To this end, the integrated optimization component is modeled as a robust variant of the Cumulative Capacitated Vehicle Routing Problem with Time Windows, where routes are constructed under uncertain travel times with an objective to minimize the total latency of deliveries (i.e., the overall waiting time of customers, which can negatively affect their satisfaction). We demonstrate the proposed LMD system's utility through real-world trials in a university campus with a single robotic courier. Implementation aspects as well as the findings and practical insights gained from the deployment are discussed in detail. Lastly, we round up the contributions with numerical simulations to investigate the scalability of the developed mathematical formulation with respect to the number of robotic vehicles and customers.

Index Terms—Last-mile Logistics, Autonomous Delivery Robot, Contactless Delivery, Vehicle Routing Problem, Robust Optimization, Pedestrian Trajectory Prediction, Surface Roughness Estimation.

I. INTRODUCTION

THE unparalleled rise of e-commerce activities over the past decade coupled with continually increasing urbanization have notably hiked the volume of urban freight logistics, especially in the last leg of distribution from suppliers to customers, known as the last-mile delivery (LMD). Within the overall chain, LMD holds the key to customer satisfaction, yet is notoriously cumbersome and inefficient due mainly to: (1) lack of automation; (2) inconsistent and congested delivery routes; (3) consumers' elevated expectation for same-day delivery. These setbacks render LMD as the most expensive

*Both authors contributed equally to this work.

This work was supported by the Khalifa University of Science and Technology under Award No. CIRA-2020-286.

E. Shaklab, A. Sharma, M. Mebrahtu, M. Basri, M. Nagy, M. Khonji, and J. Dias are with the EECS Department, Khalifa University, Abu Dhabi, UAE. (e-mails: {eyad.shaklab, arjun.sharma, murad.mebrahtu, mustofa.basri, mohamed.nagy, majid.khonji, jorge.dias}@ku.ac.ae)

A. Karapetyan is with the EECS Department, Khalifa University, Abu Dhabi, UAE, and with the Division of Engineering, New York University Abu Dhabi. (e-mail: areg.karapetyan@nyu.edu)

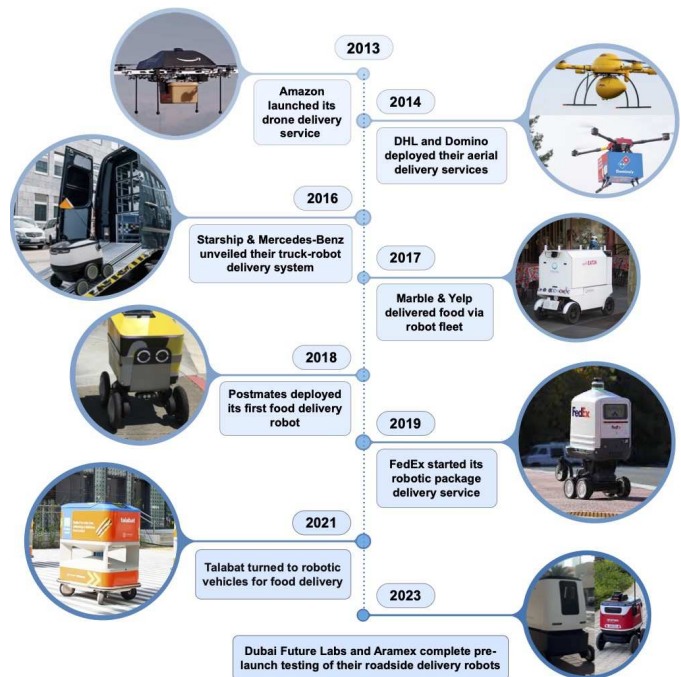


Fig. 1: Examples of real-world deployed unmanned LMD services in chronological order since 2013. The observed trend shifts from drone-based approaches to ground vehicles.

step in the supply chain, accounting for up to 53% of the total shipment cost [1]. In response, substantial efforts, both in academia and industry, have been invested into the search for more sustainable, optimized, and economic parcel delivery concepts and services [2].

While deployment of unmanned LMD modes was somewhat limited prior to COVID-19 pandemic, practitioners report an unprecedented surge in autonomous delivery services since the virus hit. Case in point, a San Francisco-based firm Starship Technologies in 2021 celebrated its one-millionth autonomous delivery and in 2022 upped the number to over 3 millions [3]. Added to that, logistic giants like DHL and UPS, aiming to future-proof their business, have recently begun active operational trials of electric delivery robots and vehicles [4], [5]. In fact, according to a recent Gartner report [6], the number of robotic LMD couriers operated worldwide is estimated to reach to one million by 2026.

As summarized in Fig.1, early attempts of automating parcel deliveries relied primarily on unmanned aerial vehicles (UAVs), commonly known as drones. Admittedly, off-the-shelf

drones are agile, swift, low-cost and are being increasingly utilised throughout the globe as a means to streamline monitoring, inspection, mapping, and environmental surveillance procedures [7]. However, their operation in urban areas is accompanied by several challenges and negative byproducts, such as noise pollution, privacy and security concerns, and no-fly zone restrictions [8]. As experimentally demonstrated in [9], drones are energy-efficient specifically for transportation of lightweight packages and could be useful in rural regions, whereas for urban environments ground robots tend to be relatively more energy-saving. Evidently, as deduced from Fig. 1, the preference for ground-based option has prevailed over time, becoming the mainstream model of LMD robots in the market.

In developing an automated LMD system with robotic vehicles, the foremost task is to assure the robots can navigate *autonomously* and *safely* in complex dynamic environments. Currently, most of the practically operating units partially rely on remote human control or supervision (e.g., to steer around complex obstacles or halt the navigation to avoid an undetected collision) [10]. Among few exceptions is the food-tech startup Serve Robotics, which in 2022 completed commercial deliveries at Level 4 autonomy (i.e., relying solely on vehicles' onboard capabilities) [11]. It should however be noted that the company's fleet of self-driving LMD carriers is designated to travel specifically on sidewalks.

As real-world practice revealed, compared to human counterparts existing robotic LMD couriers fall short in two subtle yet essential aspects – *flexibility* and *situational inference*. In particular, users often found it inconvenient to attend to the robot for receiving the parcel instead of collecting it from the desired drop-off location [10]. This is also pertinent to current COVID-19 regulations, which endorse contactless operations. More importantly, their lack of basic inference and proactiveness (or interactiveness) with the surrounding environment can expose to otherwise avoidable risks. For instance, in 2019 an incident in Pittsburgh involving an autonomous sidewalk LMD vehicle left a wheelchair-bound individual stranded in a dangerous situation on the street after persistently blocking their passage [12]. These demerits, besides limiting the utility of robotic couriers, hinder customers' satisfaction and acceptance of automated last-mile logistic services.

Actuated by the above causes and practical insights, we design and experimentally demonstrate a *fully autonomous AI-boosted* LMD system for optimal and green logistics in urban (small) communities. The system employs self-driving ground vehicles, built on top of a commercial mobile robotic platform, which feature a *touchless* multi-parcel delivery mechanism and a *triple-layer safety stack* (people-platform-package). More concretely, the contributions and roadmap of the present work are as follows:

- 1) After surveying the related literature on robot-assisted LMD approaches in Sec. II, we proceed to formalizing the optimization problem involved in the proposed LMD system. Specifically, Sec. III formulates a robust variant of the Cumulative Capacitated Vehicle Routing Problem with Time Windows, referred to as RCCVRPTW, in which a fleet of robotic LMD carriers with varying

capacities strive to optimally meet customers' desired delivery schedules in the presence of nondeterministic delays. Here, incorporation of nondeterminism reflects the practical need to account for autonomy-induced uncertainties (e.g., sensor noise, imprecise localization) and external disturbances linked to pedestrian movements or dynamic obstacles.

- 2) Sec. IV provides an in-depth overview of the proposed framework's architecture, followed by the details of the constructed self-driving LMD carrier and its three auxiliary modules for enhanced usability and added safety: (i) A proactive audio service, hinging on a Recurrent Neural Network, for *real-time intent prediction* and early notification of pedestrians; (ii) A reactive perception system for *vibration monitoring* and parcel safety; (iii) Automatic package unloading mechanism. To facilitate reproducibility, the software implementation was based entirely on the open-source Robotic Operating System (ROS). The complete software stack can be accessed online at https://github.com/AV-Lab/AVL_segwayrmp.
- 3) To validate the effectiveness and practicality of the featured autonomous LMD system, a series of test trials were designed and carried out in the outdoor premises of a university campus. The results of preliminary deployment¹ (with one vehicle), reported in Sec.V, illustrate the merits of the proposed framework allowing the autonomous robotic courier to navigate safely and intelligently in the presence of pedestrians, cars, and dynamic obstacles. In all the case studies performed, the robot completed the autonomous deliveries with minimum total latency without violating customers' preferred time schedules. Moreover, with the newly presented parcel safety module in place, up to 40% reduction of vibrations were recorded in the robot's storage compartment. Lastly, numerical simulations are conducted to analyse the scalability of RCCVRPTW's optimization model against the number of robotic couriers and customers.

II. LITERATURE SYNOPSIS

Given the breadth of literature on last-mile logistics and associated vehicle routing problems, the following survey is confined to studies focusing on unmanned delivery systems. For a more exhaustive review on general LMD problems and approaches, the reader is referred to [28]–[30]. Depending on the pursued mode of operation, the existing studies on unmanned LMD systems can be organized under three main themes: aerial, hybrid (aerial-ground), and ground-based. In the paragraphs to follow, we survey the developments in each of these research threads, whereas Table I provides an overall comparison between the present work and the literature reviewed.

As noted in Sec. I, early approaches to automating last-mile deliveries focused primarily on drones. For instance, Dorling et al. [14] propose a drone-based LMD system and formulate different variants of multi-trip VRPs (MTVRP) that cater for

¹Video records of one of the trial runs can be accessed online at <https://youtu.be/-9Zams67hNY>.

	System Setup	Objective	Auxiliary Safety Module(s)	Field Testing	Mathematical Formulation	Delivery Time Constraints	Uncertainty
Torabbeigi et al. [13]	Drones	Minimize the number of delivery drones	—	×	Extended VRP	×	×
Dorling et al. [14]	Drones	Minimize the overall delivery time or total cost	—	×	MTVRP	×	×
Shao et al. [15]	Drones	Minimize the flight path length of the drone	—	×	BMCDRP	×	×
Huang et al. [16]	Bus + Drone	Minimize delivery time	—	×	VRP	×	✓
Mathew et al. [17]	Truck + Drones	Minimize the total delivery cost	—	×	HDP	×	×
Poikonen et al. [18]	Truck + Drones	Minimize the delivery time and return of all vehicles	—	×	VRPD	×	×
Liu et al. [19]	Truck + Drones	Minimize overall travelling cost	—	×	E2-VRP	×	×
Boysen et al. [20]	Truck + AGVs	Minimize weighted number of late deliveries	×	×	TBRD	Deadline	×
Simoni et al. [21]	Truck + AGV	Minimize delivery time	×	×	TSP-R	×	×
Chen et al. [22]	Truck + AGVs	Minimize total time spent in all routes	×	×	VRPTWDR	Time Window	×
Chen et al. [23]	Truck + AGVs	Minimize total time spent in all routes	×	×	VRPTWDR	Time Window	×
Sonneberg et al. [24]	AGV	Minimize delivery cost	×	×	ELRP-TW	Time Window	×
Buchegger et al. [25]	AGV	Parcel delivery	×	✓	—	—	—
Li et al. [26]	AGVs	Parcel delivery	✓	✓	—	—	—
Gao et al. [27]	AGV	Parcel delivery	×	✓	—	—	—
Present work	AGVs	Minimize customers' waiting time	✓	✓	RCCVRPTW	Time Window	✓

TABLE I: A summarised comparison of present work versus prior studies on unmanned LMD systems.

the effect of battery and payload weight on drones' energy consumption while also allowing multiple trips to the depot. The problems are modeled as Mixed-integer linear programs (MILPs) and tackled by the numerical optimizer CPLEX. Focusing on short-distance delivery with drones, Torabbeigi et al. [13] model the LMD problem as an extension of the Vehicle Routing Problem (VRP). The problem includes drone battery endurance and drone weight capacity as constraints. On the other hand, Shao et al. [15] envision an LMD system with battery exchange stations to extend the drone's delivery coverage range. The optimisation component within the system is defined as the Battery and Maintenance Constrained Drone Routing problem (BMCDRP) where the objectives are to minimize the delivery time and the number of landing depots on the flight path. A heuristic solution methodology based on the Ant Colony and A* algorithms is developed to find approximate solutions for BMCDRP.

Incidentally, a separate research stream has been exploring hybrid unmanned LMD systems consisting for example of drone-truck, drone-public bus, or drone-AGV combinations. By utilizing the public transportation system (public buses) and drones, Huang et al. [16] propose a hybrid LMD system for cost-effective and environmentally friendly long-distance parcel deliveries. The approach employs a Dijkstra-based method to determine the shortest route from the depot to the customer, minimizing the delivery time. Importantly, the proposed approach incorporates probabilistic edge costs to account for the uncertainty in the public transportation network. In [17], Mathew et al. present an LMD system combining a UAV and a truck for deliveries in urban environments. The truck, which is restricted to travel along a street network, transports the drone which delivers packages to customers. The problem is formulated as an optimal path planning problem on a graph, termed as Heterogeneous Delivery Problem (HDP), that falls under the category of a static VRP with coordination constraints between the vehicles. In a similar setup, Poikonen et al. [18] propose an LMD system synergising UAVs and trucks to parallelize deliveries and model the problem as a VRP with drone (VRPD). Liu et al. [19] consider an extended variant of the traditional two-echelon VRP (E2-VRP) for cooperated trucks and drones where multiple parcels can be delivered in one drone's flying route. Subsequently, a two-stage route-based heuristic approach is developed to optimize both the truck's main route and the drone's flying routes.

In support of a fully ground-based realisation, the pa-

pers in [20]–[23] studied various optimization problems for LMD systems comprising trucks/vans loaded with on-board autonomous small robots. Boysen et al. [20] propose a variant of VRP, termed as Truck-based Robot Delivery Scheduling problem (TBRD), seeking to minimize the weighted number of late customer deliveries. The studied LMD system considers a delivery truck that launches robotic delivery vehicles each intended for a single customer. The authors develop scheduling procedures that determine the truck route along with the robot depots and drop-off points where robots are launched. In [21], Simoni et al. formulate the LMD problem as an extension of TSP referred to as TSP with Robot (TSP-R). A system consisting of a truck and a robot is envisioned, where the robot is deployed by the truck during delivery stops to serve certain customers. The robot is designed to have a divisible storage compartment and can perform more than one consecutive delivery. In a similar setup, in [22] and [23], Chen et al. formulate the LMD problem as a VRP with time windows and delivery robots (VRPTWDR) where the objective is to minimize the total route duration. Time window constraints are incorporated to account for customers' availability. In view of VRPTWDR's NP-hardness, an adaptive large neighborhood search heuristic algorithm is proposed as a solution method.

Towards complete automation of last-mile logistics, several prior works developed and/or studied LMD systems based exclusively on AGVs. In [24], Sonneberg et al. frame the LMD problem as a version of VRP coined as Electric Location Routing Problem with Time Windows (ELRP-TW). In this model, customers are assigned to stations, each with its own AGV. The objective in ELRP-TW seeks to optimize the total cost by determining the optimal positioning of stations as well as route construction of AGVs. Moreover, battery, parcel weight, and volume restrictions are considered for multiple consecutive deliveries. On the applied side, Buchegger et al. [25] present an autonomous vehicle, built upon a commercially available electric vehicle (Jetflyer), for parcel delivery in urban environments. The vehicle was evaluated in two urban settings. However, the developed system employs a hierarchical first-come-first-serve approach with no optimization of delivery routes and order. In [27], Gao et al. developed a bespoke self-driving robot for last-mile deliveries. The software implementation was built upon Autoware, which is an open-source framework for autonomous driving. In [26], Li et al. present JD.com's (a large e-commerce company in China) methodological framework for autonomous last-mile deliveries

in complex traffic conditions and outline the architecture of their autonomous delivery vehicle. The vehicle features a machine learning-based perception module for recognizing generic traffic-related objects/signs and tracking dynamic obstacles in the environment (e.g., vehicles and pedestrians). To navigate safely through complex traffic conditions, the system employs a prediction module to approximate the future trajectories of the tracked moving obstacles as well as a remote monitoring and control module.

As transpires from the above review and Table I, the existing literature studied autonomous LMD systems from one specific angle, focusing either on the underlying mathematical optimization model or the technical and implementation aspects of self-driving robotic vehicles. To close this gap, we unify these two constituents into a coherent LMD system, thereby enabling end-to-end automation and optimization of the logistic process. In turn, practical insights gained during the implementation and deployment served to inform the mathematical modeling of the optimization component as reflected by the incorporation of non-determinism to account for autonomy-induced uncertainties and real-world externalities. Furthermore, the current study advances the existing research by introducing two new modules for refined usability and added safety, namely the reactive perception system for vibration monitoring and parcel safety and the automatic package unloading mechanism for contactless delivery.

III. PROBLEM STATEMENT

Recall that within the proposed architecture, sketched in Fig. 2, RCCVRPTW serves as a logistic planner responsible for optimizing the dispatch of contracted delivery robots such that the waiting time of all customers is minimized. The robotic couriers must depart from the central depot and visit the respective set of customers² assigned by RCCVRPTW such that collectively all the delivery requests are fulfilled. To define the problem formally, we next establish the relevant mathematical notation.

Consider a directed or undirected complete graph $\mathcal{G} = (\mathcal{V} \cup \{0\}, \mathcal{E})$, where the root 0 harbours the depot, the vertices in $\mathcal{V} \triangleq \{1, \dots, n\}$ encode customer destinations and the edge set $\mathcal{E} \triangleq \{(i, j) : i, j \in \mathcal{V} \cup \{0\}, i \neq j\}$ corresponds to the delivery routes between these nodes. Each arc $(i, j) \in \mathcal{E}$ is associated with a duration $d_{i,j}$ that measures the robotic vehicles' travel time while traversing from site i to j . To synthesize a logistic planner that is robust against non-determinism stemming from unknown parameters or external disruptions (e.g., imprecise localization, sensor noise, number of encounters with pedestrians), we model $d_{i,j}$ as a stochastic, yet bounded, parameter with a box uncertainty set of the form $\mathcal{U} = \{d_{i,j} \in \mathbb{R}_+ : |d_{i,j} - \bar{d}_{i,j}| \leq \epsilon\}$, where $\bar{d}_{i,j}$ denotes the *nominal travel time* and $\epsilon \in \mathbb{R}_+$ is a preset constant. A user-selected time interval $[s_i, f_i]$ is imposed on every vertex $i \in \mathcal{V}$, with s_i and f_i specifying the earliest and latest times the delivery service at node i can be performed, respectively (i.e., the availability window of a customer). Should a robotic

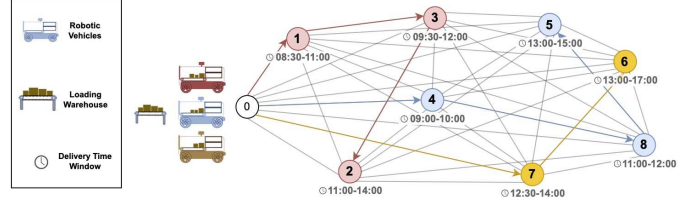


Fig. 2: An abstract illustration of the studied LMD system where a fleet of robotic couriers serve a set of customers geographically dispersed around the central depot (node 0).

courier reach vertex i prior to start time s_i , a delay occurs before the package is supplied. The *latency* l_i of node $i \in \mathcal{V}$ is defined as the total elapsed time (since departing from the depot) until the service at node i starts.

Let $\mathcal{K} \triangleq \{1, \dots, m\}$ denote the set of employed robotic couriers and $c_k \in \mathbb{Z}_+, k \in \mathcal{K}$ be their compartment capacities. Each vehicle's journey starts and ends at the central depot, however since the return trip does not influence the sought objective of minimizing the cumulative latency of deliveries, we embed \mathcal{V} with a dummy terminal node $n+1$ and write the augmented set of all vertices and edges as $\mathcal{V}^+ \triangleq \{0, 1, \dots, n\}$ and $\mathcal{E}^+ \triangleq \{(i, j) : i, j \in \mathcal{V}^+, i \neq j\}$, respectively. For each $k \in \mathcal{K}$ and $(i, j) \in \mathcal{E}^+$, define a *binary decision variable* $x_{i,j}^k$ such that

$$x_{i,j}^k = \begin{cases} 1, & \text{if vehicle } k \text{ is directed to pass through arc } (i, j) \\ 0, & \text{otherwise} \end{cases}$$

With the foregoing notation, RCCVRPTW embodies into a mixed-integer linear program of the form:

$$\min_{\mathbf{x}} \sum_{i \in \mathcal{V}} l_i \quad (\text{RCCVRPTW})$$

$$\text{s.t.} \quad \sum_{k \in \mathcal{K}} \sum_{j \in \mathcal{V}^+} x_{i,j}^k = 1, \quad \forall i \in \mathcal{V}, i \neq j \quad (1)$$

$$\sum_{j \in \mathcal{V}^+} x_{i,j}^k = \sum_{j \in \mathcal{V}^+} x_{j,i}^k, \quad \forall k \in \mathcal{K}, i \in \mathcal{V}, i \neq j \quad (2)$$

$$\sum_{j \in \mathcal{V}} x_{0,j}^k \leq 1, \quad \forall k \in \mathcal{K} \quad (3)$$

$$\sum_{i \in \mathcal{V}} x_{i,n+1}^k \leq 1, \quad \forall k \in \mathcal{K} \quad (4)$$

$$\sum_{k \in \mathcal{K}} \sum_{j \in \mathcal{V}^+} x_{n+1,j}^k = 0, \quad (5)$$

$$\sum_{k \in \mathcal{K}} \sum_{i \in \mathcal{V}^+} x_{i,0}^k = 0, \quad (6)$$

$$\sum_{i \in \mathcal{V}^+} \sum_{j \in \mathcal{V}^+ : j \neq i} x_{i,j}^k \leq c_k, \quad \forall k \in \mathcal{K} \quad (7)$$

$$l_i - l_j + Mx_{i,j}^k \leq M - d_{i,j}, \quad \forall k \in \mathcal{K}, i \neq j \in \mathcal{V} \quad (8)$$

$$l_0 - l_j + Mx_{0,j}^k \leq M - d_{0,j}, \quad \forall k \in \mathcal{K}, j \in \mathcal{V} \quad (9)$$

$$l_i - l_{n+1} + Mx_{i,n+1}^k \leq M - d_{i,n+1}, \quad \forall k \in \mathcal{K}, i \in \mathcal{V} \quad (10)$$

$$l_0 = d_{i,n+1} = 0, \quad \forall i \in \mathcal{V} \quad (11)$$

$$l_{n+1} \geq 0, \quad (12)$$

$$s_i \leq l_i \leq f_i, \quad \forall i \in \mathcal{V} \quad (13)$$

$$x_{i,j}^k \in \{0, 1\}, \quad \forall i, j \in \mathcal{V}^+, k \in \mathcal{K} \quad (14)$$

$$d_{i,j} \in \mathcal{U} \quad \forall (i, j) \in \mathcal{E}, \quad (15)$$

²Each customer is visited once and the delivery service can be performed only within specific customer-defined time windows.

where M stands for a sufficiently large positive constant. Given the fleet of available robotic couriers, RCCVRPTW is targeted at finding the corresponding set of optimal delivery routes that minimize the aggregate waiting time of customers. In the above formulation, which was extended from [31], Constrs. (1)-(6) resemble a multi-commodity network flow; Constr. (1) ensures all the customers are serviced exactly once, Constr. (2) guarantees that a vehicle arriving at a node will also leave that node, Constrs. (3) to (6) assert that a robotic vehicle's trip originates from the depot and ends at the dummy terminal node, and each vehicle can be scheduled for at most one trip. The robotic carriers' capacity limits in terms of the number of packages are expressed through the constraint in (7). Constrs. (8) to (9) model the compatibility requirements between routes and schedules, acting as subtour elimination constraints. Lastly, the bilateral inequality in (13) enacts customers' preferred time windows and Constrs. (10) and (11) cater for the added dummy variables.

When the robotic fleet is reduced to a single uncapacitated vehicle and edge traversal times are deterministic, RCCVRPTW simplifies to the Traveling Repairman Problem with Time Windows (TRPTW) [32]. As a special case of the TSP, the TRP (i.e. a TRPTW with time windows dropped) falls within the class of NP-hard problems and has been studied in the literature under various different names, including Minimum Latency Problem [33], Traveling Repairman Problem [34], Delivery Man Problem [35] and Cumulative Traveling Salesman Problem [36]. Unlike TSP and VRP, where the objective is to minimize the total time required to visit all customers, TRP and CCVRP seek to minimize the cumulative waiting time of customers (i.e., service latency). In a sense, the latter problems take a *customer-centric perspective* rather than a cost-oriented view as in TSP, hence the choice of cumulative latency as an objective function in RCCVRPTW.

IV. FULLY AUTONOMOUS LMD SYSTEM

This section details the developed LMD system, which appears in Fig. 3, and its components, each elaborated in a separate subsection.

A. System Overview

The proposed autonomous LMD system comprises four main components: (1) the optimal logistic tour planner that computes the minimum latency dispatch routes of robotic vehicles (Sec. III); (2) the vibration monitoring module (VMM) which dynamically modulates vehicles' speed based on the roughness of the driving surface to reduce vibrations (Sec. IV-E); (3) the autonomous navigation stack responsible for obstacle avoidance as well as for constructing the global and local paths (Sec. IV-C); (4) the proactive AI pipeline which caters for an additional layer of human safety and aids reducing deviations and interruptions in vehicles' set course of travel (Sec. IV-D).

B. Robotic LMD Courier

The featured robotic vehicle was assembled by retrofitting the commercial mobile platform Segway RMP 440. The

platform is integrated with four lithium phosphate battery modules that maintain the 12-hour endurance of the vehicle. The maximum speed of the robot with a full payload of 100 kg is 29 km/hr. The material used to fabricate the enclosure compound is Poly (methylmethacrylate) (a.k.a Acrylic) and the aluminum L-angles are reinforced with Acrylic to provide further rigidity to the structure. At the front of the vehicle, an external ancillary battery bank enclosed with a tilt lift cover mechanism with hot-swap capability is installed to power the added equipment. As detailed below, the enclosure volume is divided into a computer and electronics zone, and package and conveyor zone.

- 1) Computer and electronics zone: The total power requirement of the system is 485 W under normal conditions, and 650 W at peak. This zone accommodates the computing unit, sensors, and the inverter module. The employed computer requires 24 V, 20 A to operate. The sensors are safeguarded by several relays and in-line fuses. Step-up/step-down transformers are utilized to regulate the voltage and current for all the sensors, motors, micro-controller, and motor controllers. A power inverter outputting a 3 KW pure sine waveform is installed to support accessories that run on alternating currents.
- 2) Package and conveyor zone: The unloading mechanism relies on a conveyor belt driven by a DC motor which can support up to 8 kg of load. Three packages of dimensions 200mm x 200mm x 200mm can be fit onto the belt. The contactless delivery is achieved via a two-fold ramp mechanism that extends the ramp length twice. The ramp is unfolded at an angle, and the package slides over to the ground. The delivery process of a single parcel takes less than 20 seconds. The choice of the current unloading setup owes primarily to its simplicity and cost, whereas for future deployments the mechanism can be substituted by a robotic arm-based retrieving mechanism that can detect and place the intended package on the ramp.

As Fig. 3 depicts, the vehicle is equipped with a 2D LiDAR (Hokuyo UTM-30LX), 3D LiDAR (Velodyne Puck Lite), stereo camera (Stereolabs ZED 2), and an IPC (Nuvo 8108GC-XL Industrial PC). The IPC can operate at high ranges of ambient temperature and humidity as well as withstand extensive shock and vibrations, which duly suits the current deployment environment in Abu Dhabi. The 3D LiDAR, which is part of the vehicle localization system, was utilized due mainly to its long detection range (100 m) and could have been replaced with a 2D alternative with a comparable range since only a single laser scan layer was processed. The positioning of the bottom LiDAR was set in order to capture curbs and otherwise overlooked low obstacles, effectively allowing to avoid computationally intensive cloud/laser filtering or surface segmentation techniques. For an effective implementation of the VM module (Sec. IV-E), we avail an additional 3D LiDAR placed at the front of the vehicle at an inclination of 15 degrees with respect to the ground, which allows capturing the immediate in-front driving surface. The Zed 2 camera, which

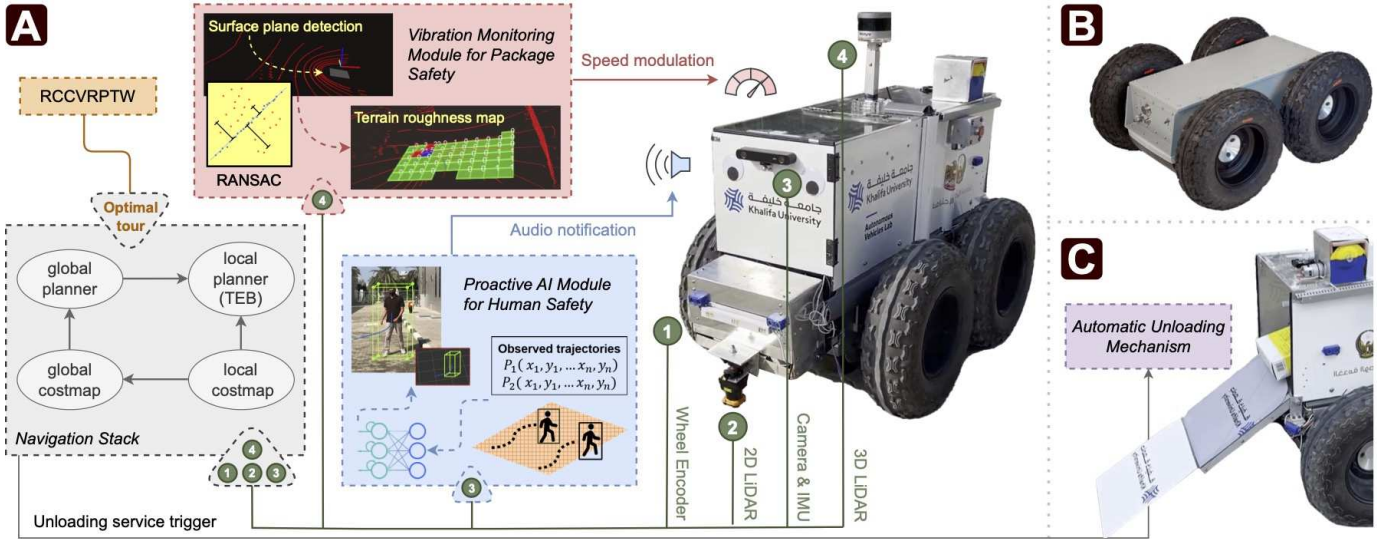


Fig. 3: Infographic overview of the constructed fully autonomous LMD carrier prototype and its functionalities: A) The retrofitted vehicle and its key components; B) The bare-bone RMP 440 platform; C) Contactless multi-parcel delivery mechanism.

supports spatial object detection and features an in-built IMU, was employed to complement the autonomous navigation stack and the proactive AI module for human safety (Sec. IV-D).

C. Autonomous Navigation and Platform Safety Stack

The assembled navigation stack operates based on the time-series sensor readings received from the LiDARs, IMU, and wheel encoders as illustrated in Fig. 3. Prior to deployment, the operational area of the system was mapped to generate the global costmap, which is a two-dimensional representation of static obstacles in the environment. The global planner takes as an input a set of way-points produced by RCCVRPTW (i.e., the optimal logistic sequence) and processes the set iteratively, activating the automatic unloading mechanism whenever the corresponding navigation goals are reached. For local path planning, we resort to the Time-Elastic-Band (TEB) algorithm; a decision taken under extensive experimentation with existing planners in ROS, such as the Dynamic Window Approach (DWA) and the base local planner. TEB relies on the local costmap generated from real-time LiDAR readings to design locally optimal paths allowing for collision-free navigation among detected static and dynamic obstacles. However, the default parameters of the local and global planners in ROS may require judicious fine-tuning to satisfy the desired risk tolerance level and use-case specifics. Since in the current LMD system platform safety is prioritised, we adjust the parameters in a conservative manner as detailed in Sec. V-A.

D. Proactive AI Pipeline for Human Safety

To reinforce the human safety component within the proposed LMD system, we develop an AI-boosted proactive module to predict pedestrians' trajectories and minimize the risk of collisions. Pedestrian trajectory prediction is an extensively researched topic that has been studied for various

applications, including pedestrian safety, human-tracking, and crowd surveillance. The challenge here lies primarily in the complexity of human motion, which conventionally was modeled via physics-based approaches with handcrafted techniques [37]–[39]. Although successful to an extent, such methods are limited in their representation and scalability [40]. Most recent trajectory prediction methods resort to deep learning (DL) techniques, which allow to alleviate some of the challenges faced with handcrafted methods. Recurrent Neural Network (RNN) is one of the prevalent DL methods in the literature on trajectory prediction. RNNs are commonly used to predict sequential data such as trajectory. Its more advanced variant, known as the Long Short-term Memory (LSTM) network, have gained traction as an efficient method for pedestrian trajectory prediction in complex, dynamic scenes [41]–[43].

For the purposes of the current study, we employ the model proposed in [43] referred to as Bi-directional Pedestrian Trajectory Prediction with Multi-modal Goal Estimation Model (BiTrap). BiTrap is a goal-oriented conditional variational autoencoder hinging on an RNN-based trajectory prediction model. Thanks to the inbuilt advanced bi-directional decoder,

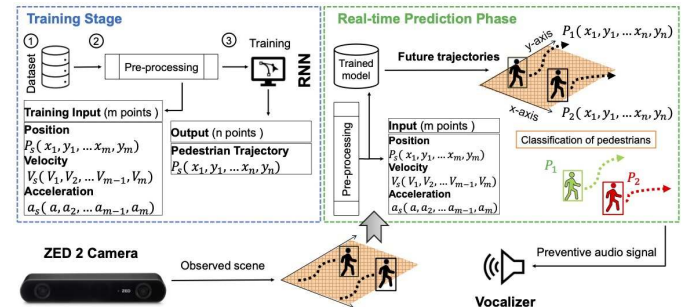


Fig. 4: A summary of the proposed proactive human safety pipeline with trajectory prediction and vocalizer.

BiTrap allows for long-term trajectory prediction. As an input, the model takes pedestrians’ observed trajectories as well as motion data such as velocities and accelerations.

In the proposed module, the ZED 2 camera depicted in Fig. 4 was employed to detect, locate, and track pedestrians. Particularly, bounding boxes of all pedestrians in the field of view of the camera are extracted. These boxes contain the 3D coordinates of the pedestrians in reference to the camera. The tracked information is saved as observed trajectories, which are then fed to BiTrap. Following the related works in [41]–[45], 8 data points from a pedestrian’s observed trajectory are taken as input, and 12 data points are generated as output. Depending on the predicted trajectories of pedestrians and their observed distances (from the vehicle) a preventive audio signal is produced via a ROS service (dubbed vocalizer). Here, the audio message serves as an early notification to pedestrians, intending to circumvent potential collisions with the vehicle as well as minimize interruptions/deviations in the vehicle’s set course of navigation.

For the sake of analysis, we classify pedestrians into three categories: red, blue, and green. The red category highlights pedestrians that are in a dangerously close-proximity to the vehicle as determined by a preset threshold. Pedestrians in blue are those whose future trajectory predicted by BiTrap model collides with the vehicle’s planned path (unless the speed or trajectory of the pedestrian changes). The green category is for pedestrians who are at a safe distance from the vehicle and no collision is foreseen. The vocalizer is set to react for blue and red classes.

E. Vibration Monitoring Module for Package Safety

When dispatched on uneven terrains, robotic vehicles may endure vibrations that could result in damage to the vehicle’s hardware or the packages carried. While suspension systems can alleviate these concerns, they require dedicated hardware, which can add complexity and cost. Furthermore, installing such systems may not be possible in some situations, or might not be worth the investment if the vehicle generally drives on an even terrain and only occasionally encounters rough patches or segments. Generally, the severity of the vibrations that a robotic vehicle sustains is directly related to its speed. Therefore an effective way to improve both the safety of the vehicle and the packages it carries is to modulate its speed based on the roughness of the driving surface.

Some relevant research work in this area concentrates on road cracks and pothole detection. Anand and Gupta [46] presented an end-to-end DL approach to detect road cracks by texture and spatial features on the image. The approach employs Seg-Net [47], [48] for semantic segmentation to extract road pixels, followed by a neural network to detect cracks. On the other hand, Aggarwal and Jain [49] resort to basic image processing algorithms to capture cracks and potholes.

Detecting cracks and potholes on a driving surface provides only a partial understanding of its condition since it doesn’t reflect the overall smoothness of the ground. To address this limitation, we leverage a LiDAR to generate a 3D grid map

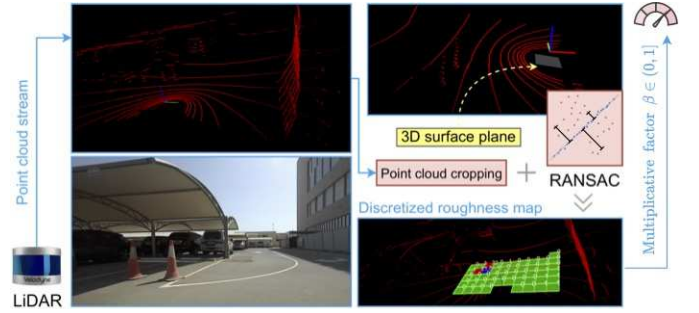


Fig. 5: Illustration of the proposed Vibration Monitoring module with speed modulation. Point cloud data from a 3D LiDAR is parsed through RANSAC to detect the surface plain, based on which the discretized roughness map is constructed in real time.

that captures the surface roughness more accurately. Initially, the LiDAR’s point cloud is cropped to cover the area in front of the vehicle. Then, the RANSAC algorithm [50] is invoked to obtain a 3D plane of the driving surface. The algorithm iteratively generates various plane parameters and selects the best one fitting the highest portion of the given point cloud. We then quantify the surface roughness by measuring the perpendicular Euclidean distance between each impact point on the surface and the fitted plane. Since the LiDAR’s point cloud resolution is not sufficiently high, we split the surface into smaller boxes ($1\text{m} \times 1\text{m}$) and compute the average roughness in that area. The calculated roughness score can be utilised in two ways: (1) It can be embedded into the navigation stack as a local cost map, allowing the local planner to generate a path that passes through the lowest cost boxes while adjusting speed if necessary; (2) Alternatively, only the boxes directly in front of the wheels’ orientation can be considered and the vehicle’s speed can be adjusted based on the roughness of those boxes. Overall, this module creates a trade-off between speed and ride quality that can be fine-tuned depending on the application specifics.

In the proposed method, overviewed in Fig. 5, we sample the boxes two meters directly in front of the robotic vehicle. The boxes with roughness scores from 0 to 5 cm are highlighted in green as an indication of a smooth surface. The boxes highlighted in blue represent a moderate roughness with a score between 5 to 20 cm, whereas rough surfaces with a score higher than 20 cm are colored in red. These thresholds were determined based on real-world experiments on various driving surfaces and can be adjusted based on the adopted platform and application. The VMM throttles the vehicle’s speed by a multiplicative factor $\beta \in (0, 1]$ according to the computed average score of these regions. For high roughness scores, we set $\beta = 0.5$, while for moderate and low roughness $\beta = 0.75$ and $\beta = 1$ were considered, respectively.

V. FIELD TESTS AND SIMULATION STUDIES

To test the effectiveness and practicality of the proposed autonomous LMD system, a series of real-world trial experiments were conducted in which the robotic courier presented in Sec. IV was deployed to deliver packages to five customers

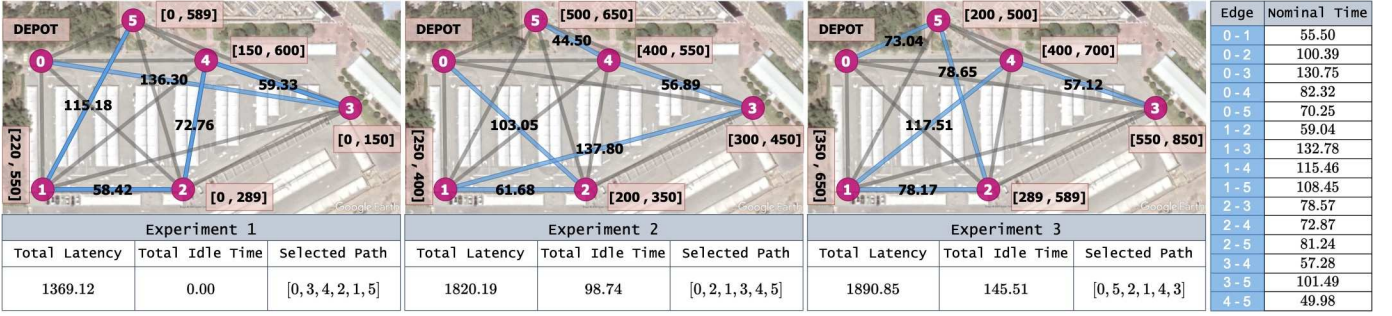


Fig. 6: Visualized results of the performed real-world experiments. The edges highlighted in blue represent the optimal path selected by RCCVRPTW. The numbers on the edges encode the actual travel time (in seconds) of the robotic vehicle during the experiments, while the table on the right lists the estimated nominal times.

autonomously. Video footage of some of the test runs is available online³. Complementary to these real-world tests, in Sec. V-C simulation studies are provided to examine the scalability of RCCVRPTW’s MILP model established in Sec. III with respect to the number of vehicles and customers.

A. Setup and Scenarios of Trial Experiments

The first set of experiments were performed in Khalifa University’s staff parking lot. The area is around 10,000 square meters, and contains shaded parking slots that are in clusters around the middle. The parking lot is paved and routinely maintained and features mixed traffic of vehicles and pedestrians. The area mapping was performed with a Simultaneous Localization and Mapping (SLAM) package that is based on OpenSlam’s Gmapping particle filter. Gmapping provides a laser-based 2D SLAM solution to produce a 2D occupancy grid map from laser and pose data collected by the vehicle, the vehicle was driven around the perimeter and in between the parking lot sections to generate this occupancy grid. To facilitate the global path planning within the autonomous navigation stack, the global occupancy grid was manually edited to highlight the parking areas, sidewalks around the perimeter of each parking cluster, as well as sidewalks around the perimeter of the whole lot; these low features were not properly captured by the 3D LiDAR, which was placed in a high vantage point in order to produce a reliable occupancy grid for localization. If the occupancy grid was used without editing, the global planner would produce paths that often would overlap with untraversable areas. Although the local planner can adjust the path dynamically on-the-fly to bypass newly detected unmapped obstacles, the resulting trajectories would likely be jagged and more lengthy. For enhanced safety of robotic carriers, the autonomous navigation stack parameters in ROS were tuned as follows. The buffer (inflation) zone of obstacles was set to 1 meter, the maximum speed was set to 1.2 m/s, and the local costmap dimension was set to 6x6 meters.

One can observe from Fig. 3 that the current implementation does not rely on GPS for localisation or navigation. The integration of the GPS data into the vehicle’s pose proved no

noticeable improvement while adding more computational and hardware requirements. This owes mainly to the characteristics of the testing area, which was feature dense and yielded sufficiently accurate localisation results with LiDAR. In addition, a GPS-less solution would prove more useful since it could be extended into areas with unreliable GPS coverage or GPS-denied environments such as indoor locations.

The delivery nodes were allocated in the corners of the parking lots as portrayed in Fig. 6. To determine the pairwise nominal travel time between the nodes (to be inputted to RCCVRPTW) the vehicle was autonomously driven 10 times along each edge (in both directions) and the average value was taken. As one demonstration, the proposed autonomous LMD solution is tested on three scenarios with varying delivery time preferences. In the first scenario, the opening time windows of the customers are mostly relaxed (i.e., large time ranges where customers accept deliveries), while the second and third had stricter temporal constraints. To discern between the results, the corresponding experiments are labeled **E1** to **E3**. For each experiment, the vehicle’s optimal logistic route was obtained by invoking the Gurobi optimizer on the respective MILP program of RCCVRPTW. The site in which the first set of experiments were conducted is well paved and routinely maintained, thus in order to investigate the proposed VMM’s performance two additional experiments, labeled **E4** and **E5**, were conducted (which are summarized in Fig. 8). These new experiments were performed in a different area that featured an unpaved and uneven sandy terrain. The LMD vehicle was autonomously driven in a 50 meters straight path. The VMM’s speed modulating parameter was set to $\beta = 0.75$ when the ground’s estimated roughness value falls in-between 5 and 20 cm.

B. Results

1) *LMD Performance*: As evidenced by Fig. 6, the customers’ delivery schedules (i.e., time windows) were respected in all the experiments. There was no idle time in **E1**, where **E2** and **E3** had 98.74 and 145.51 seconds of idle time, respectively. It is to be noted that idle time is not incorporated into the objective function of the current formulation. For future investigations, a bi-objective optimization problem can be considered to additionally minimize idle time. The actual

³<https://youtu.be/-9Zams67hNY>

traversal time in **E1** to **E3** differs from the estimated nominal time, which is due to stochastic factors such as pedestrian movements and sensor noise. This substantiates the need to account for uncertainties in the formulation. In the experiments performed, the observed deviations fell within the range (± 5 seconds) as evidenced by Fig. 6.

2) *Package Safety*: The results of **E4** and **E5** are highlighted in Fig.8, the plot shows the linear acceleration readings from the LMD vehicle’s IMU in the X, Y, and Z axes. **E4** shows the readings with the VMM disabled, while **E5** displays the readings with the VMM enabled. It is observed that with the VMM disabled, there are more spikes in the IMU’s readings, and the intensity of the vibrations is higher than compared with the VMM being enabled. Since there is no speed modulation in **E4**, the vehicle took 50 seconds to traverse the 50-meter straight path autonomously, compared with the 62 seconds in **E5** where the VMM was frequently engaging to throttle the speed based on the roughness estimates computed by the perception system. This yielded around 40% decrease in the magnitude of vibrations.

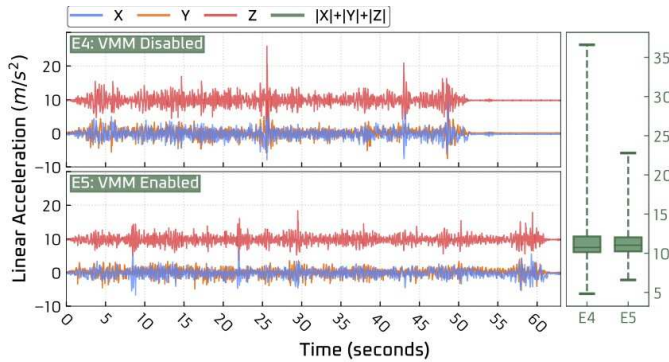


Fig. 8: Comparison of the recorded vibrations in **E4** (VMM disabled) and **E5** (VMM enabled). The right-most subplot displays the range of vibration values in each experiment.

3) *Real-time Intent Prediction and Early Notification of Pedestrians*: In this section, we provide a qualitative and quantitative analysis of the developed proactive AI Pipeline for human safety based on the results of **E3**, video footage of which is available online (<https://youtu.be/-9Zams67hNY>). The experiment was performed in a relatively less crowded

parking lot, however, various interaction scenarios were captured.

As mentioned in Sec. IV-D, we discern pedestrian bounding boxes into three color-coded classes: green, blue, and red. The green box indicates a pedestrian being at a safe distance with no collision predicted in the near future. The blue class indicates a pedestrian being at a safe distance from the vehicle, but their predicted trajectory and the near future trajectory of the vehicle might collide. Lastly, the red bounding box signifies an imminent danger of collision with the vehicle, due mainly to the proximity of the pedestrian to the vehicle.

In **E3**, the vehicle had five total instances of interactions with pedestrians: three with single pedestrians, one with two pedestrians, and one with a group. Since trajectory prediction is a continuous process, we evaluate the developed predictive model by dividing each interaction into three distinct phases. The first phase assigns a class label to the pedestrian after initial detection, using the aforementioned green, blue, and red bounding boxes. The second phase assigns a label to the pedestrian halfway through the interaction, based on their predicted behavior and trajectory. The third and final phase assigns a label just before the pedestrian leaves the view or vicinity of the vehicle. Interactions refer to the time from pedestrian detection to the moment when they are no longer within 20 meters of the vehicle.

The results of the experiment are listed in Table II. In the first interaction, a pedestrian initially positioned around 15 meters from the vehicle moved further away. As anticipated, the module labels the pedestrian green throughout the interaction interval. In the second interaction, a pedestrian initially moves towards the vehicle and then stops on the vehicle’s path while it continues approaching. The proactive module labels the pedestrian as safe at first since the pedestrian was far away and hinted signs of moving left. When the pedestrian was

Interaction	Number of pedestrians	Detected Pedestrians	Class Label	Expected Label
1	1	1	G-G-G	G-G-G
2	1	1	G-B-R	G-B-R
3	3+	2	G-G-G	G-G-G
4	1	1	R-B-G	R-B-G
5	2	2	G-B-G	G-B-G

TABLE II: Performance of the adopted BiTrap model for inferring pedestrians’ future trajectories. The three labels (G - Green, B - Blue, and R - Red) delimited by dashes (e.g., G-B-G) represent the class labels in the three phases of interaction.



Fig. 7: Snippets of a pedestrian interaction with the vehicle during **E3**: A) The pedestrian moves dangerously close to vehicle. B) The pedestrian moves towards the vehicle’s path C) The pedestrian moves away from the vehicle.

standing still the output label started alternating between green and blue. This is because the observed trajectory for a standing pedestrian does not provide sufficient context on their future intention. After a while, however, the pedestrian’s position became too close to the vehicle and therefore the red label was assigned. In the third interaction, a group of pedestrians were standing on the left side of the vehicle in a shaded parking. Due to poor visibility, only two of the three were detected. Since all of them were standing in a safe distance, they were labeled green.

In the fourth interaction, illustrated in Fig. 7, a pedestrian approached the vehicle from the right side and was labeled red due to their close proximity (less than 0.5 meters). As the pedestrian moved away, the label turned blue since their path still intersected with the vehicle’s planned trajectory. Eventually, the pedestrian moved further away, resulting in a change of their classification to green. During the final interaction, two pedestrians emerged on the right side of the vehicle and were labeled as green. As they approached the vehicle and seemed to be crossing its path, their labels changed to blue. However, they eventually came to a stop without crossing the vehicle’s path, and the label changed to green.

C. Scalability Analysis

In view of practical limitations, RCCVRPTW instances considered in the above-reported field tests were confined to a single vehicle and 5 nodes (customers). To shed light on the empirical computational cost of RCCVRPTW for higher-dimensional inputs, this section analyzes the results of numerical simulations (summarized in Fig. 9) with up to 37 customers and 10 robotic LMD couriers. The simulations were coded in Python and carried out on an Intel i9-9900k CPU.

We evaluate the presented MILP model’s performance through a series of simulations based on two different sets of instances. In the first case study, the results of which appear on the leftmost two subplots in Fig. 9, RCCVRPTW’s output is analyzed on a set of 50 randomly generated synthetic instances with $n = 11$ customers and vehicle capacities set to $c_k = \lceil 2 \cdot \frac{n}{|\mathcal{K}|} \rceil, \forall k \in \mathcal{K}$, considering $|\mathcal{K}|$ being varied from 2

to 10 in steps of 2. The second case study, visualised in the rightmost subplot of Fig. 9, investigates the model’s scalability with respect to the number of nodes on 5 instances⁴, generated by Potvin and Bengio [51] from Solomon’s RC2 VRPTW benchmark set, where $|\mathcal{K}|$ was set to 6 and $c_k = 10, \forall k \in \mathcal{K}$.

As Fig. 9 indicates, when applied to RCCVRPTW the solver’s execution time does not scale linearly with the problem size and may vary significantly depending on the instance data. While for the RC2 instances, the running time did not exceed 10 seconds, in the case of random instances with an equal number of LMD vehicles ($|\mathcal{K}| = 6$) the execution time averaged approximately to 200 seconds. On the positive side, the observed running time decreased drastically as the fleet size $|\mathcal{K}|$ increased (since the instance complexity is more relaxed). We remark that for large-scale instances with more than 40 customers, solving RCCVRPTW optimally can be intractable. In such situations, one can resort to efficient heuristic/meta-heuristic approaches such as the Hybrid Genetic Search algorithm proposed in [52].

VI. CONCLUSION

Aiming to inform and advance the design of effective autonomous last-mile logistic systems, we developed and experimentally demonstrated a customer-centric, fully-autonomous LMD system for small urban communities. The presented system relies on self-driving robotic vehicles, which are boosted with three auxiliary modules for enhanced usability and added safety: (1) A proactive audio service for real-time intent prediction and early notification of pedestrians; (2) A reactive perception system for vibration monitoring and parcel safety; (3) A contactless multi-package delivery mechanism. The results of proof-of-concept operation tests illustrate the effectiveness of the proposed system in providing fully-autonomous parcel delivery services while minimizing the latency of deliveries. In all the field tests conducted, the developed autonomous robotic courier navigated safely and intelligently in the presence of pedestrians, cars and dynamic obstacles. One promising extension is to integrate the proactive AI module and the reactive perception system within the navigation stack planners to allow for more optimised planning of ‘local’ delivery paths. Additionally, future work includes extending the proposed system to the setting with cooperative LMD robots as well as incorporating battery recharging and energy constraints.

REFERENCES

- [1] S. Dolan, “The challenges of last mile delivery logistics and the tech solutions cutting costs in the final mile,” Business Insider, Jan 2022. [Online]. Available: bit.ly/3XZmEd3
- [2] R. van Duin, B. Enserink, J. Dalemán, and M. Vaandrager, “The near future of parcel delivery: Selecting sustainable solutions for parcel delivery,” in *Sustainable City Logistics Planning: Methods and Applications*. Nova Science Publishers, 2020, pp. 219–252.
- [3] I. Lunden, “Starship technologies raises another \$42m to fuel the growth of its fleet of self-driving delivery robots,” TechCrunch, Mar 2022. [Online]. Available: bit.ly/3k9Zzhz
- [4] D. Edwards, “DHL begins trial runs of Cleveron’s autonomous delivery vehicle,” Robotics and Automation News, Sep 2022. [Online]. Available: bit.ly/3YEE1kb

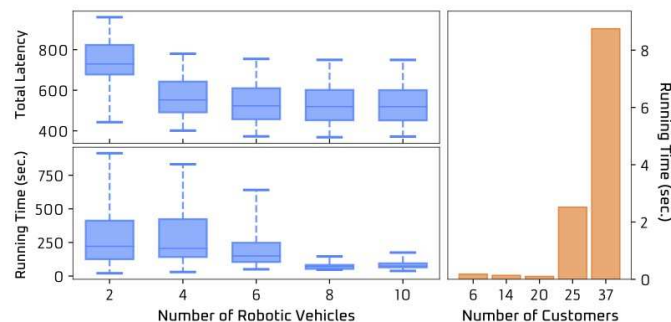


Fig. 9: Performance of the Gurobi solver on higher-dimensional instances of RCCVRPTW. The subplots on the left depict the recorded running time and objective value against the number of robotic vehicles. The rightmost subplot reports the runtime against the number of nodes.

⁴{RC_204.3, RC_207.4, RC_205.1, RC_203.1, RC_202.1}

- [5] A. Hawkins, "UPS is buying thousands of electric vans and teaming up with Waymo to accelerate the future of delivery," *The Verge*, Jan 2020. [Online]. Available: [bit.ly/3YXuhS1](https://www.theverge.com/2020/1/22/21988887/ups-waymo-delivery)
- [6] D. Klappich, S. Tunstall, C. Titze, A. Stevens, and T. Payne, "Predicts 2022: Supply chain technology," *Gartner Research*, Nov 2021. [Online]. Available: [bit.ly/3xBmqOg](https://www.gartner.com/en/newsroom/press-releases/2021-11-18-gartner-predicts-2022-supply-chain-technology)
- [7] R. Alyassi, M. Khonji, A. Karapetyan, S. C.-K. Chau, K. Elbassioni, and C.-M. Tseng, "Autonomous Recharging and Flight Mission Planning for Battery-Operated Autonomous Drones," *IEEE Transactions on Automation Science and Engineering*, pp. 1–13, 2022.
- [8] B. Sah, R. Gupta, and D. Bani-Hani, "Analysis of barriers to implement drone logistics," *International Journal of Logistics Research and Applications*, vol. 24, pp. 1–20, 06 2020.
- [9] T. Kirschstein, "Comparison of energy demands of drone-based and ground-based parcel delivery services," *Transportation Research Part D: Transport and Environment*, vol. 78, p. 102209, 2020.
- [10] D.-a. Durbin, "Robots hit the streets as demand for food delivery grows," Nov 2021. [Online]. Available: <https://bit.ly/3fB3Rku>
- [11] P. Mehar, "Serve robotics' sidewalk robot completes deliveries at level 4 autonomy," Jan 2022. [Online]. Available: <https://bit.ly/3fB3Rku>
- [12] E. Ackerman, "Why tech needs more designers with disabilities," *Bloomberg*, Nov 2019. [Online]. Available: [bit.ly/3kldCcj](https://www.bloomberg.com/news/articles/2019-11-14/why-tech-needs-more-designers-with-disabilities)
- [13] M. Torabbeigi, G. J. Lim, and S. J. Kim, "Drone delivery scheduling optimization considering payload-induced battery consumption rates," *Journal of Intelligent & Robotic Systems*, vol. 97, no. 3, pp. 471–487, Mar 2020.
- [14] K. Dorling, J. Heinrichs, G. G. Messier, and S. Magierowski, "Vehicle routing problems for drone delivery," *IEEE Transactions on Systems, Man, and Cybernetics: Systems*, vol. 47, no. 1, pp. 70–85, 2017.
- [15] J. Shao, J. Cheng, B. Xia, K. Yang, and H. Wei, "A novel service system for long-distance drone delivery using the "ant colony+a*" algorithm," *IEEE Systems Journal*, vol. 15, no. 3, pp. 3348–3359, 2021.
- [16] H. Huang, A. V. Savkin, and C. Huang, "Drone routing in a time-dependent network: Toward low-cost and large-range parcel delivery," *IEEE Transactions on Industrial Informatics*, vol. 17, pp. 1526–1534, 2021.
- [17] N. Mathew, S. L. Smith, and S. L. Waslander, "Planning Paths for Package Delivery in Heterogeneous Multirobot Teams," *IEEE Transactions on Automation Science and Engineering*, vol. 12, no. 4, pp. 1298–1308, 2015.
- [18] S. Poikonen, X. Wang, and B. Golden, "The vehicle routing problem with drones: Extended models and connections," *Networks*, vol. 70, pp. 34–43, 8 2017.
- [19] Y. Liu, Z. Liu, J. Shi, G. Wu, and W. Pedrycz, "Two-echelon routing problem for parcel delivery by cooperated truck and drone," *IEEE Transactions on Systems, Man, and Cybernetics: Systems*, vol. 51, no. 12, pp. 7450–7465, 2021.
- [20] N. Boysen, S. Schwerdfeger, and F. Weidinger, "Scheduling last-mile deliveries with truck-based autonomous robots," *European Journal of Operational Research*, vol. 271, no. 3, pp. 1085–1099, 2018.
- [21] M. D. Simoni, E. Kutanoglu, and C. G. Claudel, "Optimization and analysis of a robot-assisted last mile delivery system," *Transportation Research Part E: Logistics and Transportation Review*, vol. 142, p. 102049, 2020.
- [22] C. Chen, E. Demir, and Y. Huang, "An adaptive large neighborhood search heuristic for the vehicle routing problem with time windows and delivery robots," *European Journal of Operational Research*, vol. 294, pp. 1164–1180, 2021.
- [23] C. Chen, E. Demir, Y. Huang, and R. Qiu, "The adoption of self-driving delivery robots in last mile logistics," *Transportation Research Part E: Logistics and Transportation Review*, vol. 146, p. 102214, 2021.
- [24] M.-O. Sonneberg, M. Leyerer, A. Kleinschmidt, F. Knigge, and M. H. Breitner, "Autonomous unmanned ground vehicles for urban logistics: Optimization of last mile delivery operations," 2019.
- [25] A. Buchegger, K. Lassnig, S. Loigge, C. Mühlbacher, and G. Steinbauer, "An Autonomous Vehicle for Parcel Delivery in Urban Areas," in *2018 21st International Conference on Intelligent Transportation Systems (ITSC)*, 2018, pp. 2961–2967.
- [26] B. Li, S. Liu, J. Tang, J.-L. Gaudiot, L. Zhang, and Q. Kong, "Autonomous last-mile delivery vehicles in complex traffic environments," *Computer*, vol. 53, no. 11, pp. 26–35, 2020.
- [27] F. Gao, Y. Cheng, M. Gao, C. Ma, H. Liu, Q. Ren, and Z. Zhao, "Design and implementation of an autonomous driving delivery robot," in *2022 41st Chinese Control Conference (CCC)*, 2022, pp. 3832–3837.
- [28] N. Giuffrida, J. Fajardo-Calderin, A. D. Masegosa, F. Werner, M. Steudter, and F. Pilla, "Optimization and machine learning applied to last-mile logistics: A review," *Sustainability*, vol. 14, no. 9, 2022.
- [29] P. D. Neghabadi, K. E. Samuel, and M.-L. Espinouse, "Systematic literature review on city logistics: overview, classification and analysis," *International Journal of Production Research*, vol. 57, no. 3, pp. 865–887, 2019.
- [30] G. D. Konstantakopoulos, S. P. Gayialis, and E. P. Kechagias, "Vehicle routing problem and related algorithms for logistics distribution: a literature review and classification," *Operational Research*, vol. 22, no. 3, pp. 2033–2062, Jul 2022.
- [31] R. Van der Meer, *Operational control of internal transport*, 2000, no. 1.
- [32] J. N. Tsitsiklis, "Special cases of traveling salesman and repairman problems with time windows," *Networks*, vol. 22, no. 3, pp. 263–282, 1992.
- [33] A. Archer, A. Levin, and D. P. Williamson, "A Faster, Better Approximation Algorithm for the Minimum Latency Problem," *SIAM Journal on Computing*, vol. 37, no. 5, pp. 1472–1498, 2008.
- [34] J. N. Tsitsiklis, "Special cases of traveling salesman and repairman problems with time windows," *Networks*, vol. 22, no. 3, pp. 263–282, 1992.
- [35] M. Fischetti, G. Laporte, and S. Martello, "The delivery man problem and cumulative matroids," *Operations Research*, vol. 41, no. 6, pp. 1055–1064, 1993.
- [36] L. Bianco, A. Mingozzi, and S. Ricciardelli, "The traveling salesman problem with cumulative costs," *Networks*, vol. 23, no. 2, pp. 81–91, 1993.
- [37] D. Helbing and P. Molnár, "Social force model for pedestrian dynamics," *Phys. Rev. E*, vol. 51, May 1995.
- [38] Z. Chen, L. Wang, and N. H. C. Yung, "Adaptive human motion analysis and prediction," *Pattern Recognition*, vol. 44, no. 12, p. 2902–2914, dec 2011.
- [39] K. Yamaguchi, A. C. Berg, L. E. Ortiz, and T. L. Berg, "Who are you with and where are you going?" in *Proceedings of the 2011 IEEE Conference on Computer Vision and Pattern Recognition*, ser. CVPR '11. USA: IEEE Computer Society, 2011, p. 1345–1352.
- [40] N. Nikhil and B. T. Morris, "Convolutional neural network for trajectory prediction," in *ECCV Workshops*, 2018.
- [41] A. Gupta, J. Johnson, L. Fei-Fei, S. Savarese, and A. Alahi, "Social gan: Socially acceptable trajectories with generative adversarial networks," 2018.
- [42] A. Alahi, K. Goel, V. Ramanathan, A. Robicquet, L. Fei-Fei, and S. Savarese, "Social lstm: Human trajectory prediction in crowded spaces," in *Proceedings of the IEEE Conference on Computer Vision and Pattern Recognition (CVPR)*, June 2016.
- [43] Y. Yao, E. Atkins, M. Johnson-Roberson, R. Vasudevan, and X. Du, "Bitrap: Bi-directional pedestrian trajectory prediction with multi-modal goal estimation," *IEEE Robotics and Automation Letters*, vol. 6, no. 2, pp. 1463–1470, 2021.
- [44] Z. Yin, R. Liu, Z. Xiong, and Z. Yuan, "Multimodal transformer networks for pedestrian trajectory prediction," in *Proceedings of the Thirtieth International Joint Conference on Artificial Intelligence, IJCAI-21*. International Joint Conferences on Artificial Intelligence Organization, 8 2021, pp. 1259–1265.
- [45] A. Rasouli, I. Kotseruba, T. Kunic, and J. K. Tsotsos, "Pie: A large-scale dataset and models for pedestrian intention estimation and trajectory prediction," *2019 IEEE/CVF International Conference on Computer Vision (ICCV)*, pp. 6261–6270, 2019.
- [46] S. Anand, S. Gupta, V. Darbari, and S. Kohli, "Crack-pot: Autonomous road crack and pothole detection," 2018.
- [47] A. Kendall, V. Badrinarayanan, and R. Cipolla, "Bayesian segnet: Model uncertainty in deep convolutional encoder-decoder architectures for scene understanding," 2016.
- [48] V. Badrinarayanan, A. Handa, and R. Cipolla, "Segnet: A deep convolutional encoder-decoder architecture for robust semantic pixel-wise labelling," 2015.
- [49] G. Aggarwal and S. Jain, "Road crack detection and segmentation for autonomous driving," in *2019 International Conference on Communication and Electronics Systems (ICES)*, 2019, pp. 198–202.
- [50] T. Fujiwara, T. Kamegawa, and A. Gofuku, "Evaluation of plane detection with ransac according to density of 3d point clouds," 2013.
- [51] J.-Y. Potvin and S. Bengio, "The vehicle routing problem with time windows part ii: Genetic search," *INFORMS Journal on Computing*, vol. 8, no. 2, pp. 165–172, 1996.
- [52] T. Vidal, "Hybrid genetic search for the cvrp: Open-source implementation and swap* neighborhood," *Computers & Operations Research*, vol. 140, p. 105643, 2022.